Biochimica et Biophysica Acta 1828 (2013) 896–905

Contents lists available at SciVerse ScienceDirect

Biochimica et Biophysica Acta

journal homepage: www.elsevier.com/locate/bbamem

Interplay of mycolic acids, antimycobacterial compounds and pulmonary surfactant membrane: A biophysical approach to disease

Marina Pinheiro [a], Juan J. Giner-Casares [b], Marlene Lúcio [a], João M. Caio [c], Cristina Moiteiro [c], José L.F.C. Lima [a], Salette Reis [a,*], Luis Camacho [b]

[a] REQUIMTE, Departamento de Ciências Químicas, Faculdade de Farmácia, Universidade do Porto, Portugal
[b] Departamento de Química Física y Termodinámica, Universidad de Córdoba, Spain
[c] Centro de Química e Bioquímica, Departamento de Química e Bioquímica, Faculdade de Ciências, Universidade de Lisboa, Portugal

ARTICLE INFO

Article history:
Received 26 April 2012
Received in revised form 14 September 2012
Accepted 19 September 2012
Available online 26 September 2012

Keywords:
Anti-tuberculosis drug
Brewster angle microscopy
Langmuir monolayer
Mycolic acid
Polarization-modulation infrared reflection spectroscopy
Pulmonary surfactant

ABSTRACT

This work focuses on the interaction of mycolic acids (MAs) and two antimycobacterial compounds (Rifabutin and *N′*-acetyl-Rifabutin) at the pulmonary membrane level to convey a biophysical perspective of their role in disease. For this purpose, accurate biophysical techniques (Langmuir isotherms, Brewster angle microscopy, and polarization-modulation infrared reflection spectroscopy) and lipid model systems were used to mimic biomembranes: MAs mimic bacterial lipids of the *Mycobacterium tuberculosis* (MTb) membrane, whereas Curosurf® was used as the human pulmonary surfactant (PS) membrane model. The results obtained show that high quantities of MAs are responsible for significant changes on PS biophysical properties. At the dynamic inspiratory surface tension, high amounts of MAs decrease the order of the lipid monolayer, which appears to be a concentration dependent effect. These results suggest that the amount of MAs might play a critical role in the initial access of the bacteria to their targets. Both molecules also interact with the PS monolayer at the dynamic inspiratory surface. However, in the presence of higher amounts of MAs, both compounds improve the phospholipid packing and, therefore, the order of the lipid surfactant monolayer. In summary, this work discloses the putative protective effects of antimycobacterial compounds against the MAs induced biophysical impairment of PS lipid monolayers. These protective effects are most of the times overlooked, but can constitute an additional therapeutic value in the treatment of pulmonary tuberculosis (Tb) and may provide significant insights for the design of new and more efficient anti-Tb drugs based on their behavior as membrane ordering agents.

1. Introduction

Tuberculosis (Tb) is an infectious disease caused by *Mycobacterium tuberculosis* (MTb) and represents a major health concern around the world [1]. Nearly nine million new cases are estimated each year, two million of them being fatal due to the increment of multidrug resistant Tb [2,3]. The eradication of Tb is difficult since MTb lipidic envelope confers impermeability to antibiotics and ability to withstand unfavorable conditions [1,3,4]. For this reason, the treatment of Tb is associated to a multidrug combination therapy for at least 6 months [1]. Therefore, to improve the therapeutic compliance, new and more effective drugs are urgently needed [1,5], requiring their development new approaches to understand the mechanism of action of classical therapies.

In pulmonary Tb, which is the most common manifestation of Tb, the inhaled MTb encounters the pulmonary surfactant (PS) before reaching its target (the alveolar macrophage) [6]. Besides being a physiological barrier to the entrance of bacteria in the body, PS is from a biophysical point of view, a lipid monolayer containing hydrophobic and hydrophilic proteins. This compressible monolayer possesses a fundamental role in decreasing alveoli surface tension, which has proved to be essential to facilitate respiratory work and prevent alveoli collapse [7,8]. The recent accepted mechanism for this latter crucial function states that, during expiration, the fluid lipids and proteins with less ability to sustain high surface pressures are squeezed out from the PS monolayer, leading to an enrichment of the film with less fluid lipids [9]. During respiratory movements the lost lipids and proteins are stored in surface-associated “reservoirs” at the adjacent interface being available for further re-adsorption [10–12].

The MTb cell wall is extremely rich in lipids, and this high lipid content is consistent with the bacteria primary location nearby the air/water interface of PS monolayers. The lipids from MTb cell wall have

Abbreviations: BAM, Brewster angle microscopy; DPPC, Dipalmitoylphosphatidylcholine; DPPG, Dipalmitoylphosphatidylglycerol; LC, Liquid-condensed; LE, Liquid-expanded; LUVs, Large unilamellar vesicles; LPC, Lysophosphatidylcholine; MAs, Mycolic acids; MTb, *Mycobacterium tuberculosis*; RFB, Rifabutin; RFB2, *N′*-acetyl-rifabutin; PE, Phosphatildylethanolamine; PG, Phosphatidylglycerol; PhS, Phosphatildylserine; PI, Phosphatildylinositol; PM-IRRAS, Polarization-modulation infrared reflection spectroscopy; PS, Pulmonary surfactant; SM, Sphingomyelin; SP, Surfactant protein; Tb, Tuberculosis

* Corresponding author at: REQUIMTE, Departamento de Ciências Químicas, Faculdade de Farmácia, Universidade do Porto, Rua de Jorge Viterbo Ferreira no 228, 4050–313 Porto, Portugal. Tel.: +351 220428672; fax: +351 226093483.
E-mail address: shreis@ff.up.pt (S. Reis).

0005-2736/$ – see front matter © 2012 Elsevier B.V. All rights reserved.
http://dx.doi.org/10.1016/j.bbamem.2012.09.015

been further implicated in the PS dysfunction that causes the typical symptoms of pulmonary Tb, namely the decrease of pulmonary compliance manifested as breathing difficulty and, consequently, as an increased respiratory work [1,13]. In this regard, Chimote and coworkers have previously proposed a biophysical explanation to some of the symptoms observed in pulmonary Tb. According to these authors, the pulmonary symptoms might be due to the biophysical impairment of the lung surfactant function due to the interfacial presence of mycobacterial lipids [14]. In another study performed by the same authors, it was demonstrated by atomic force microscopy (AFM) that mycobacterial lipids could aggregate within PS monolayers, resulting in a disturbed monolayer surface activity. The authors also suggested that this could be a mechanism of lung surfactant dysfunction in pulmonary Tb [13]. Wang et al. also studied the inhibitory effects of mycobacterial lipids in bovine and calf lung surfactant models and concluded that the bacterial lipids inhibited the monolayer surface activity in both PS models [15].

Besides the importance of PS as a lung reservoir for MTb, the lungs are also organs of anti-Tb drugs bioaccumulation, possibly due to their distribution at the PS lipid level. In this context, it is important to pursue biophysical studies to unveil the interplay of antimycobacterial compounds and MTb with PS lipid monolayers, as these studies might provide additional and important insights about the therapeutic role of the drugs protecting PS monolayers from the impairment effects of the mycobacterial lipid [1,16].

To our knowledge, there is only one experimental study reported in the literature concerning the interaction of anti-Tb drugs and PS. This study performed by Chimote et al. evaluates the interactions between DPPC, the main compound of the PS, and the anti-Tb drugs (isoniazid, rifampicin and ethambutol). The results of this study have shown that the antimycobacterial compounds improve the surface parameters of the PS model, which correlates with a putative protective role of these antimycobacterial compounds of the PS biophysical integrity *in vivo* [17].

Beyond the abovementioned studies, the knowledge of the biophysical effects of both MTb membrane lipids and anti-Tb drugs is still scarce, particularly the information related with their accessibility to the PS lipid monolayer. In this context, our study provides the first comprehensive survey of the implications caused by different amounts of mycobacterial lipids in a natural lung surfactant that mimics the human PS, and it is also the first study on the interaction of RFB (RFB) and *N′*-acetyl-Rifabutin (RFB2) with PS monolayer in the presence and absence of mycobacterial lipids.

RFB is a second-line drug used in Tb treatment [1,5]. Despite being a second-line drug, RFB has shown to be more efficient than first-line drugs, such as rifampicin [18]. Moreover, RFB therapeutic value is increasing due to its beneficial effect on the newly diagnosed multidrug resistant Tb and in the prevention of the disseminated *Mycobacterium avium* complex infection in HIV positive cases [18,19]. For these mentioned reasons, and given the excellent penetration capacity of RFB in cells, as well as the accumulation of this drug in the pulmonary tissue, the biophysical study proposed herein may prove important to broaden the knowledge of this drug mechanism of action or to conduct the design of more effective derivates. In this context, our newly synthesized RFB derivate is also object of the current study (Fig. 1). In comparison to RFB, RFB2 shows better *in vitro* and *in vivo* therapeutic index, thereby being a promising drug for the clinical application in Tb treatment [5]. RFB and RFB2 were both used in this work at concentrations that were reported as effective against MTb and *Mycobacterium avium* complex and as non-toxic against Vero cells [5].

The biophysical approach of our study required not only a rational choice of the anti-Tb drugs, but also a careful choice of lipids and lipid models to mimic the biological environment encountered by these drugs. In this regard, the mycolic acids (MAs) have been chosen to mimic the MTb membrane since they are the main components of the MTb cell wall, being indispensable for its structural integrity [20,21]. MAs are α-alkyl-β-hydroxyl high molecular weight fatty acids. Each molecule consists of a hydrophobic long saturated 2-alkyl branch and a hydrophilic head group (containing the groups COOH and OH) as shown in Fig. 1 [20,22,23]. MAs occur in the cell wall of MTb as variable mixtures of different classes (α-MA, methoxy-MA and keto-MA) that exhibit different conformations in the PS monolayers [24–26]. Both keto- and methoxy-MA produce the so-called "W" conformation, with the alkyl chains folded to give four parallel arms with the carbonyl and methoxy groups hydrated by water molecules in the surface layer [22]. However, independently of the surface pressures applied, keto-MA retains the compact W-shape, while methoxy-MA adopts extended structures [22]. In the case of α-MA, the most abundant form of MAs, as the surface pressure is increased by compression, the molecules apparently change from the compact W-shape to extended conformations with two hydrocarbon chains [22,27,28]. Curosurf®, a PS porcine extract, was elected as the PS model because it presents a composition and biophysical properties similar to the human PS, being used as replacement therapy in several human disorders related to lung's injury, such as the respiratory distress syndrome [9,29]. Despite the similarities with the human PS, Curosurf® possesses a different amount of components and lacks neutral lipids and hydrophilic proteins [29]. The main component of Curosurf® is dipalmitoylphosphatidylcholine (DPPC) (Fig. 1) (47% w/w). The other prevailing lipids are zwitterionic such as lysophosphatidylcholine (LPC), sphingomyelin (SM), phosphatildylethanolamine (PE), and a significant amount of negatively charged lipids (5.7–9.6% w/w) namely phosphatidylglycerol (PG), phosphatildylinositol (PI) and phosphatilserine (PhS) [29,30]. The hydrophobic proteins present in Curosurf® are surfactant protein B (SP-B) (0.4% w/w) and SP-C (0.7% w/w), which extensively interact with the surfactant phospholipids and increase their ability to efficiently decrease the surface tension [9,29]. These proteins are cationic due to the positively charged arginine and lysine amino acids present in their composition [31,32].

In summary, besides unveiling the mechanisms of interaction of antimycobacterial compounds (RFB and RFB2) with PS (Curosurf®), this work can contribute to identify novel biophysical mechanisms that explain the therapeutic effect of these antimycobacterial compounds, hence allowing the future development of more effective drugs that are able to protect the PS monolayer from the biophysical impairment effect induced by the MAs. Additionally, and besides many studies have proven the importance of SP-B and SP-C on the function of the lung activity [10,11,31,33–35], this is the first report of the effects of MAs and antimycobacterial compounds in SP-B and SP-C studied *in situ*.

2. Materials and methods

2.1. Materials

RFB was isolated from Mycobutin® and further purified as described previously [5]. RFB2 was obtained from RFB, using a selective acylation of the secondary amine [5]. MAs were purchased from BioClot GmbH, Germany, and used without any further purification. Curosurf® was purchased from Angelini Farmacêutica Lda, Portugal, and was used as originally supplied. Sodium chloride, monopotassium phosphate and dipotassium phosphate (99% pure) were purchased from Panreac®. Chloroform and methanol were used as co-spreading solvents. The subphase used, phosphate buffer 100 mM (pH 7.4; 100 mM of sodium chloride), was prepared from ultrapure water, produced by Millipore Milli-Q unit (resistivity = 18.2 MΩ cm).

2.2. Methods

2.2.1. Langmuir trough

Two different troughs models, a KN-1005 (KSV Instruments Ltd, Helsinki, Finland) and NIMA 601(Nima Technology, Coventry, England) were equipped with two symmetrical barriers and a Wilhelmy type dynamometric system using a strip of filter paper. KN-1005 is

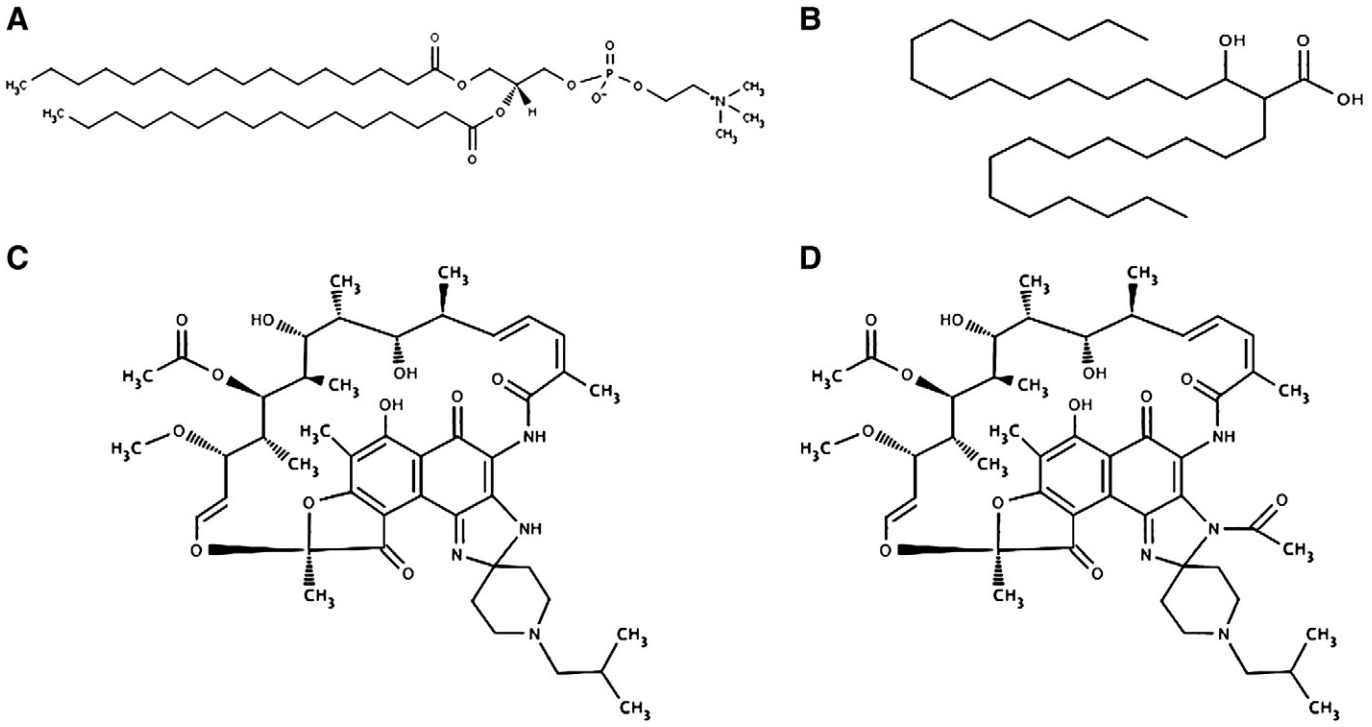

Fig. 1. Chemical structures of DPPC (A), MAs (B), RFB (C) and RFB2 (D).

nearly 325 mL in subphase volume and close to 587 cm^2 total area. NIMA 601 is about 400 mL in subphase volume with a total area close to 600 cm^2. KN-1005 was used in PM-IRRAS experiments. Due to its larger capacity and area, that allows the compensation of pressure restrictions imposed by the smaller trough [29], NIMA 601 was used to obtain the represented isotherms.

2.2.2. Film spreading

All films were prepared by spreading samples on the phosphate buffer subphase. Films were spread by deposition of tiny droplets of samples uniformly on the air–water interface, using a 250 μL microsyringe. Curosurf® was spread from 0.2 mg/mL chloroform-extracted solutions. MAs were spread from 0.2 mg/mL chloroform: methanol-extracted solutions (9:1 v/v). After spreading, solvent was allowed to evaporate for 15 min prior to film compression. The effect of antimycobacterial compounds was evaluated by spreading Curosurf®, Curosurf®:MAs (9:1 w/w) and Curosurf®:MAs (1:1 w/w) monolayers on a phosphate buffer with a known concentration of RFB and RFB2 (0.118 μM and 0.225 μM respectively).

2.2.3. Film compression

All spread films were compressed at a rate of 20 cm^2/min (at a much slower rate than the respiratory movements, due to experimental limitations). During compression, surface pressure–area isotherms (π/A) were recorded until the maximum compression possible in our trough (*i.e.* at the maximum value of ≈50 mN/m of compression). The absolute molecular area ($Å^2$/molecule) of DPPC was used to express the compression isotherms. All experiments were performed in an atmosphere with 100% relative humidity at 21 °C.

2.2.4. Brewster angle microscopy

Brewster angle microscopy (BAM) images were obtained from a I-Elli 2000 apparatus (supplied by Nanofilm Technologies, Goettingen, Germany) using a Nd:YAG diode laser, which can be recorded with a lateral resolution of 2 μm. The image processing procedure included a geometrical correction of the image, as well as a filtering operation to reduce interference fringes and noise. Furthermore, the brightness of each image was scaled to improve contrast.

2.2.5. Polarization-modulation infrared reflection spectroscopy

Polarization-modulation infrared reflection spectroscopy (PM-IRRAS) was performed using a KSV PMI 550 instrument (KSV Instruments Ltd, Helsinki, Finland) recording the spectra every 2 mN/m from 0 to 40 mN/m. The Langmuir trough was set up so that the light beam reached the monolayer at a fixed angle of incidence of 80°. The incoming light was continuously modulated between s and p polarization at a high frequency. This allowed the simultaneous measurements of spectra for the two polarizations, and their difference provides surface-specific information, while their sum provides the reference spectrum (buffer with or without antimycobacterial compound). In this work, PM-IRRAS was elected due to the advantages over the conventional IRRAS mode, namely the independence of modulated reflectivity of the isotropic adsorption from the vapor or bulk water, overcoming the problem of the surrounding water vapor [36,37].

2.2.6. Parameters studied from the surface pressure–area Langmuir isotherms

A variety of systems have been used for determining the surface activity of surfactant materials derived from the lungs, including Langmuir trough and captive bubble surfactometer [38–41]. In comparison to the Langmuir trough, the captive bubble surfactometer reveals a much lower compressibility, extremely low surface tensions and a moderated hysteresis if the film collapse is avoided [42]. However, over the past few years, the evolution of Langmuir trough designs allowed it to sustain high surface pressures which, coupled with spectroscopy and image techniques such as BAM and IRRAS, constitutes a valuable system to visualize the morphology and the characterization of the PS monolayers [9,40]. Langmuir isotherms give information about the lipid phases and the phase transitions, which are both dependent on the temperature, the pressure, and the pH [43,44]. The parameters studied from the surface pressure–area (π/A) Langmuir isotherms were: the minimum area per molecule; the hysteresis and the

compressibility. The minimum area per molecule (A_{min}) is the mean area occupied for one molecule in the surface layer and it indicates the molecular packing and the interactions between the monolayer components. This parameter was determined by extrapolation of a line tangent to the condensed region. Hysteresis was acquired by the monolayer compression/decompression isotherms and corresponds to the difference between compression and decompression areas [32]. The cycle of compression/decompression was performed to mimic the expiration/inspiration movements, respectively. Elastic modulus (C_s^{-1}) was calculated from the π/A isotherms by the following equation: $C_s^{-1} = -A\,(d\pi/dA)$, where A is the area per lipid molecule, and π is the surface pressure. C_s^{-1} describes the relationship between the surface pressure increase and the area per molecule decrease. A higher value of C_s^{-1} is indicative of a less compressible monolayer [44,45].

3. Results and discussion

3.1. Comparison of compression isotherms

Fig. 2 represents the pressure–area (π/A) isotherm of Curosurf®. In the recorded isotherm three biophysical states of the PS monolayer can be identified: zone A, zone B and zone C [43]. The molecular nature of these three regions is further discussed in the BAM and IRRAS measurements. The zone A of the Curosurf® isotherm, between 0 and 5 mN/m, represents a less ordered region with high compressibility, typical of a liquid-expanded (LE) phase of the monolayer [12]. In the LE phase, phospholipid acyl chains have a considerable degree of rotational freedom. The zone B, between 5 and 40 mN/m, corresponds to a less compressible film and represents the coexistence of two phases: liquid-condensed (LC) and LE phase. The Curosurf® isotherm did not show an apparent phase transition plateau but the appearance of a plateau region (zone C) starting at ≈43 mN/m is noticeable. In this region, before and after reaching the plateau, natural surfactant films have lower compressibility due to the removal of the LE phase from the film by the "squeezing-out" of the proteins and fluid lipids like PGs, that leave the interface and consequently lead to the monolayer enrichment with DPPC [12,46]. In this plateau region the isotherm undergoes a monolayer-to-multilayer transition plateau, in which π only increases slowly with significant film compression [9]. The appearance of the plateau region in the 40–50 mN/m range is controversially discussed. Some authors pointed this plateau region as the film collapse [47,48]. However, other authors report a first plateau region within this pressure range and describe it as the transition of monolayer-to-multilayers [9,49]. They showed that this characteristic plateau is followed by a rapid increase in the surface pressure that leads to a second plateau (the film collapse) [9]. Indeed, in Fig. 2 it is possible to observe that after the plateau region (π above 47 mN/m) a pressure increment starts to happen, possibly leading to the monolayer collapse, which was not reached due to the maximum compression possible in our trough. *In vivo*, during the inhalation–expiration cycle, the lung surfactant monolayer experiences surface tension values between 30 and 0 mN/m [50]. However since TB starts with the inhalation of MTb, the equilibrium inspiratory surface tension (correspondent to a surface pressure of 40 mN/m) is the most relevant in this work. Additionally, in the pulmonary TB, due to surfactant deficiency and/or dysfunction, a pronounced elevated alveolar surface tension might occur [51].

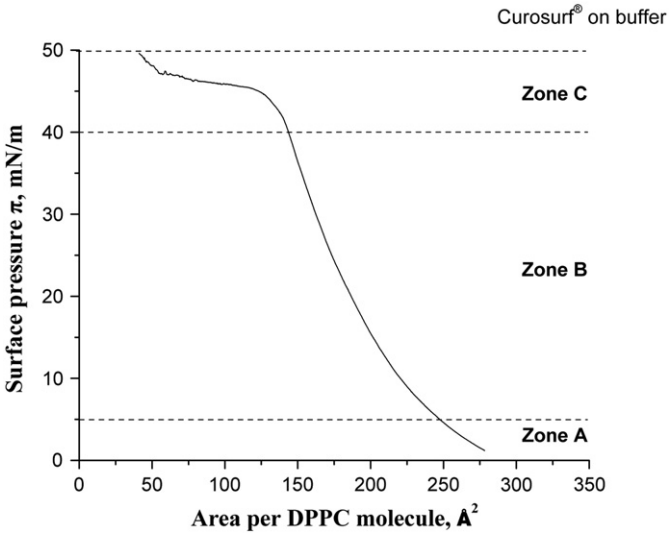

Fig. 2. Surface pressure (π/A) isotherm of Curosurf®.

The comparison between the Curosurf®:MAs (9:1 w/w) and Curosurf®:MAs (1:1 w/w) isotherms (Fig. 3) indicates that the effect of MAs on the biophysical properties of Curosurf® is concentration dependent. For lower concentrations of MAs, the biophysical effects are negligible as the isotherms Curosurf®:MAs (9:1 w/w) and Curosurf® are almost superimposed. The interactions of the Curosurf® monolayer with higher amounts of MAs are pronounced and occur at all the different regions of the isotherm. Higher amounts of MAs shift the isotherm to larger molecular areas, *i.e.* causing a monolayer expansion. At the zone C, the transition of monolayer-to-multilayer happens at the same pressure as for lower amounts of MAs, and occurs at slightly lower pressures when compared to the Curosurf® monolayer in the absence of MAs, meaning that in the presence of MAs the PS monolayer is less stable. Moreover the MAs contain negatively charged carboxyl groups at the physiological pH (predicted using MarvinView® 5.4.1.1 software from ChemAxon), and thus electrostatic repulsions with the PS head groups might happen, contributing to the monolayer expansion. Van der Waals interactions may also take place, between the mycolate alkyl chains and the PS acyl chains. Furthermore, the MAs chain-length asymmetry might create spaces through part of the lipid film thickness into which alkyl chains of associated PS phospholipids may fit, justifying the earlier transition of the PS to a more condensed phase when the MAs are present [27,52].

The antimycobacterial compounds (RFB and RFB2) clearly change the isotherm of Curosurf® (Fig. 3). The interactions with the antimycobacterial compounds are higher at the LE region (zone A) since the lower lipid density in this region facilitates the drug interaction and insertion in comparison to the LC region (zone C). Despite the very

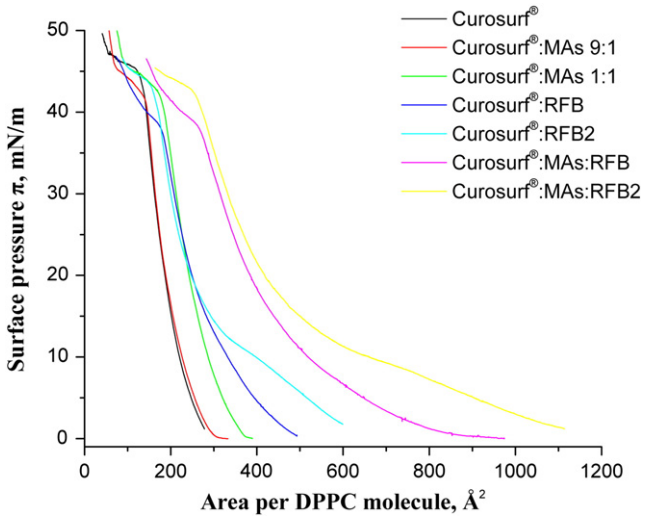

Fig. 3. Surface pressure (π/A) isotherms of Curosurf® (black line), Curosurf®:MAs 9:1 w/w (red line), Curosurf®:MAs 1:1 w/w (green line), Curosurf®:RFB (0.118 μM) (dark blue line), Curosurf®:RFB2 (0.225 μM) (light blue line), Curosurf®:MAs (1:1 w/w):RFB (0.118 μM) (purple line) and Curosurf®:MAs (1:1 w/w):RFB2 (0.225 μM) (yellow line).

similar interactions of both antimycobacterial compounds in the zones A and B, it can be observed that RFB2 interacts more extensively with the PS model. This might be due not only to the higher concentration of RFB2 used, but also to the presence of an acetyl group that confers a bulkier and an extra lipophilic group that is more prone to interact with the lipids/proteins of the PS. Moreover, the isotherm of Curosurf®:RFB2 presents a smaller plateau region at $\pi \approx 5$–10 mN/m, that is not observed in the case of Curosurf®:RFB, which represents the LE and LC phase coexistence and a more visible phase transition. The extra acetyl group of RFB2 must be once more a reason for this difference, conferring a higher surface activity that for this reason demonstrates increased ability to spread at the interface. The higher interaction of RFB2 with the PS model, comparing with RFB, might justify its previously reported higher *in vivo* efficacy [5]. This was further confirmed by the second compression isotherm of the PS model after the decompression, which has revealed to be more similar to the first compression when in presence of RFB2 than in presence of RFB (data not shown). It is possible to recognize that in the zone C the antimycobacterial compounds interact differently with the Curosurf®. In the case of RFB, the transition of monolayer-to-multilayer starts at $\pi \approx 38$ mN/m. For RFB2 the transition begins at $\pi \approx 42$ mN/m, which is slightly lower compared to the Curosurf® but higher than RFB. Since this transition occurs when the proteins and the PG lipids are "squeezed out" from the monolayer to form the multilayers [53] and at smaller pressures when in the presence of RFB, it is predictable that, in comparison to RFB2, RFB's interactions with PG and proteins are higher. According to the distribution of the charged species, predicted by MarvinView® 5.4.1.1 software from ChemAxon, at the physiological pH RFB has a higher contribution of the positively charged species (due to the ionization of the piperidine nitrogen with a pKa 9.5) [54], possibly promoting stronger electrostatic interactions with the negatively charged phospholipids (like PG).

The effect of the antimycobacterial compounds in the presence of both Curosurf® and MAs was also tested (Fig. 3). The presence of the antimycobacterial compounds and the higher quantities of MAs shifted the Curosurf® isotherm to higher areas, these changes occur in all the different regions and especially at the lower pressures for the same reasons already described. Furthermore, the transition of monolayer-to-multilayers occurs at the same pressures previously described in the isotherms of Curosurf® with the antimycobacterial compounds and in the absence of MAs.

The A_{min} determined for Curosurf® was 101 Å^2/molecule. The difference between compression and expansion isotherms is small, considering that it was only performed at the first cycle, which is essential for an efficient PS [32,43]. The maximum C_s^{-1} calculated for Curosurf® was 439 mN/m (Table 1), close to the value for pure DPPC [44,55]. As expected, the C_s^{-1} maximum values were found for surface pressures ranging from 20 to 30 mN/m, as well in the plateau region from 40 to 50 mN/m (data not shown) [55]. The A_{min} of the Curosurf® in the presence of the MAs is clearly higher. This denotes that MAs remain at the interface, probably within the PS components, under compression. The integration of MAs in the PS monolayer can occur as a result of the interactions of the MAs with the head groups or with the phospholipid tails of the lipid PS components. The interactions of the MAs with the PS head groups possibly happen by means of hydrogen bonds and electrostatic interactions, and explain the increase of the A_{min} of the Curosurf® in the presence of the MAs, as these interactions cause a large area requirement of the head group and, to optimize their van der Waals interactions, force the chains to be tilted in the condensed phase [44]. If the interactions with the phospholipid tails also take place, they would be more pronounced in the case of higher amounts of MAs. However, the value of the A_{min} is very similar in the presence of the two different proportions of the MAs studied. The intercalation of the MAs residues within the components of the PS, in order to compensate the chain-length differences and to produce higher packing density, may be the responsible for the very similar values of the A_{min} observed by higher amounts of MAs [52]. Additionally, a non-mixed monolayer may also be formed due to the lack of correlation between the MAs amount and the A_{min} and also due to the collapse pressure obtained, which is the same independently of the MAs concentration. Besides analyzing the changes induced by the MAs in the A_{min} of the PS monolayer, it is also important to study the effect of the MAs in other parameters, such as the hysteresis behavior of the PS monolayer. A good hysteresis behavior results from a small difference between the compression and expansion isotherms of the monolayer [32]. In the opposite case of higher hysteresis the interfacial work of breathing is increased [43]. MAs increase the hysteresis value of the PS monolayer and this increase reaches significantly higher values ($\approx$46%) with the higher amount of MAs. This finding is consistent with the deleterious effect caused by the MTb in the interfacial work of breathing. Regarding the effects of MAs in the C_s^{-1} of the PS monolayer, a biphasic behavior is observed. Lower amounts of MAs did not change the C_s^{-1} whereas higher amounts of MAs are responsible for a more compressible monolayer with a C_s^{-1} value lower than that obtained for the PS model in the absence of MAs. Consistent with our work, previous studies of mixed monolayers of MAs and phospholipids having a choline head group (the main phospholipids present in our PS model) reported a monolayer expansion effect (*i.e.* monolayer becomes more compressible) [14,52]. The C_s^{-1} values suggest that the MAs are integrated within the phospholipids of the monolayer, consequently causing a monolayer expansion that seems to be dependent of the MAs amount. The increase in the compressibility of the PS monolayer, as observed in the presence of MAs, has a negative connotation for the PS surface activity, as it indicates the sudden destabilization of the PS film that is related to a poorly packed surfactant and leads to an increased breathing work [51].

Both antimycobacterial compounds shift the A_{min} of Curosurf® to higher values, indicating a strong interaction of the antimycobacterial compounds with the PS. The A_{min} is higher in the presence of RFB comparing to RFB2. Although RFB2 is bulkier, this antimycobacterial compound might be located nearer to the phospholipids tails due to the presence of one extra acetyl group. RFB shallower location at the head groups of PS phospholipids is consistent with the higher A_{min}, given the large area requirement of the head groups. Both antimycobacterial compounds increase the hysteresis of the PS, being the hysteresis increase caused by RFB2 smaller ($\approx$19%) compared to the hysteresis increase caused by RFB ($\approx$36%). Overall, both RFB and RFB2 interact extensively with Curosurf® forming less compressible monolayers as observed by the increase of C_s^{-1} values. Furthermore, the interaction of the antimycobacterial compounds with "squeezed-out" components of the PS (lipids like PG and proteins) seems to happen especially for RFB, due to the lower values of the pressure of transition from monolayers to multilayers in the presence of this antimycobacterial compounds.

In the presence of MAs both antimycobacterial compounds shift the A_{min} of Curosurf® to even higher values than that observed when the

Table 1
Minimum area per lipid molecule, elastic Modulus and hysteresis of the Langmuir Curosurf®, Curosurf®:MAs 9:1 w/w, Curosurf®:MAs 1:1 w/w, Curosurf®:RFB (0.118 μM), Curosurf®:RFB2 (0.225 μM), Curosurf®:MAs (1:1 w/w):RFB (0.118 μM) and Curosurf®:MAs (1:1 w/w):RFB2 (0.225 μM) monolayers on the phosphate buffer.

	A_{min} (Å^2/molecule)	C_s^{-1} (mN/m)	Hysteresis ((Å^2/molecule)·mN/m)
Curosurf®	101 ± 5	439 ± 10	4013 ± 100
Curosurf®:MAs9:1	135 ± 5	441 ± 10	4698 ± 100
Curosurf®:MAs1:1	138 ± 5	398 ± 10	7470 ± 100
Curosurf®:RFB	198 ± 5	877 ± 10	6278 ± 100
Curosurf®:RFB2	183 ± 5	735 ± 10	4955 ± 100
Curosurf®:MAs:RFB	424 ± 5	1350 ± 100	8182 ± 100
Curosurf®:MAs:RFB2	481 ± 5	1330 ± 100	8348 ± 100

MAs were not present. The interactions of the antimycobacterial compounds with the MAs might form a bulky complex that then interacts with the negatively charged head groups of the PS justifying the great changes observed in the A_{min}. Contrastingly to the effect of the antimycobacterial compounds on Curosurf®, observed in the absence of MAs, in the presence of higher amounts of MAs, RFB2 elevates the A_{min} to higher values than RFB. This might be attributed to a closer interaction of the complex MAs and RFB2 with the head groups of the PS and consequently the greater area requirements at the head group region of the PS monolayer translate into higher A_{min} values. Both antimycobacterial compounds, in the MAs presence, increase the hysteresis of the PS (≈51%), with no noticeable differences between the effects of each antimycobacterial compound. Although in the presence of MAs the antimycobacterial compounds form less compressible PS monolayers, the increase in the C_s^{-1} values was similar to that observed when the antimycobacterial compounds were interacting with the PS monolayer in the absence of MAs.

3.2. BAM

BAM is a powerful tool that enables the visualization of the morphological changes that occur during the compression of the monolayers. Moreover, BAM also gives some information on the fluidity of the film in relation to the geometry of the domains observed at the water interface [56]. The contrast in BAM images is due to local differences in the monolayer refractivity index, caused by differences in local molecular density or packing [10,12,57].

The morphologies of Curosurf®, Curosurf®:MAs (9:1 w/w), Curosurf®:MAs (1:1 w/w), Curosurf®:RFB, Curosurf®:RFB2, Curosurf®:RFB:MAs (1:1 w/w) and Curosurf®:RFB2:MAs (1:1 w/w) at constant π of about 4, 24 and 40 mN/m (zones A, B and C) of the first compression are shown and were directly observed by BAM (Fig. 4).

The domains of Curosurf® appear at pressures above ≈24 mN/m (transition from LE to LC) and become larger with the compression, as it can be confirmed by the image obtained at 47 mN/m (Fig. 4B). For intermediate pressures ($24 \le \pi \le 40$ mN/m) the BAM images show a homogenous size distribution of circular shape lipid domains (see inset of ≈24 mN/m in Fig. 4A). For $\pi > 40$ mN/m the lipid domains are noncircular and have ramified shape domains (see inset of 47 mN/m in Fig. 4A). These lipid domains with a starry aspect are very characteristic of this natural PS [29]. Furthermore, the BAM image obtained in the plateau region (Fig. 4A) confirms that the monolayer collapse was not reached since the domains' coalescence was not observed. The BAM image appears mainly gray, which is consistent with a high fraction of solid phase. The white spots that appear on the top are attributed to the fluid phase material that is pushed out of the interface when the transition of monolayer-to-multilayer occurs and a DPPC enriched film is formed [12,57]. The presence of low amounts of MAs is enough to promote a significant change in the PS lipid domains. The transition of LE to LC occurs at $\pi \approx 3$ mN/m (data not shown), and for $\pi \approx 4$ mN/m, small elliptical domains with a very small size can be observed (Fig. 4C). The size and number of these lipid domains increase with the pressure. For all the different regions, the domains have an elliptical shape. Higher amounts of MAs promote higher differences in the lipid domains' size and morphology. For $\pi \approx 4$ mN/m some brighter points appear with a heterogeneous distribution along the predominant LE region (Fig. 4D). These brighter points might be aggregates of MAs with phospholipids, such as PI [14]. Although being more pronounced for lower pressures, the brighter points are present at all the different pressures evaluated. For intermediate pressures ($24 \le \pi \le 40$ mN/m) the lipid domains are not as visible, but it is possible to recognize the presence of some small and elliptical domains. The brighter points are also present, but in a smaller amount and with a more homogenous distribution (data not shown). For higher pressures, the presence of smaller aggregates can be observed. In the plateau region there is an enrichment of the monolayer in DPPC and the few aggregates are probably due to MAs' collapse [22,23,27,52]. Furthermore, the BAM image, for $\pi \approx 40$ mN/m (Fig. 4D), confirms the MAs' collapse, probably because MAs are less surface active in comparison to the Curosurf® components, and thus the PS and MAs mixed monolayer reaches the collapse earlier at smaller surface pressures [14].

The BAM images of Curosurf® in the presence of antimycobacterial compounds reveal the existence of very bright regions that can be associated with RFB and RFB2 local clusters with high refractive index, indicating the formation of the antimycobacterial compound at the interface (Fig. 4E and F). In the case of RFB, the antimycobacterial

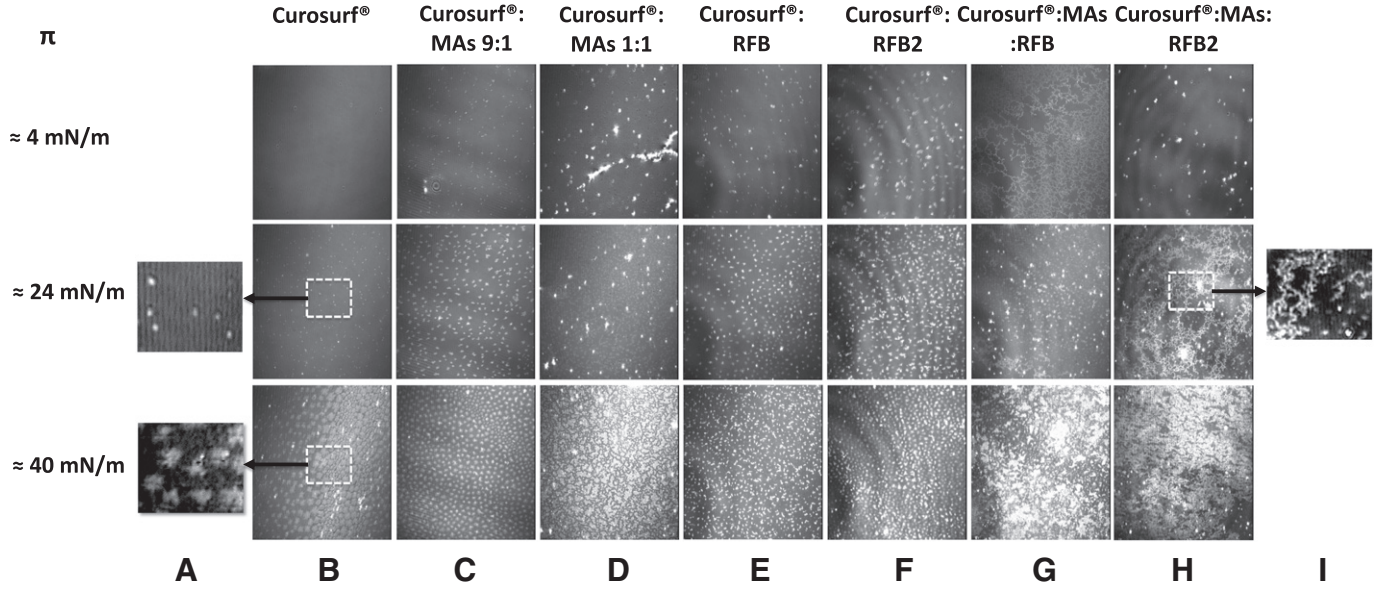

Fig. 4. BAM images of Langmuir monolayers of Curosurf® (5.3 mN/m–221 Å^2/molecule; 23 mN/m–179 Å^2/molecule; 47 mN/m–64 Å^2/molecule), Curosurf®:MAs 9:1 w/w (6.1 mN/m–248 Å^2/molecule; 25 mN/m–173 Å^2/molecule; 45 mN/m–80 Å^2/molecule), Curosurf®:MAs 1:1 w/w (3.7 mN/m–332 Å^2/molecule; 25.6 mN/m–225 Å^2/molecule; 45 mN/m–115 Å^2/molecule), Curosurf®:RFB (0.118 μM) (4.4 mN/m–404 Å^2/molecule; 26.5 mN/m–220 Å^2/molecule; 47 mN/m–74 Å^2/molecule, Curosurf®:RFB2 (0.225 μM) (6.1 mN/m–488 Å^2/molecule; 24.4 mN/m–220 Å^2/molecule; 43.6 mN/m–152 Å^2/molecule, Curosurf®:MAs (1:1 w/w):RFB (0.118 μM) (6.6 mN/m-600 Å^2/molecule; 24.7 mN/m-346 Å^2/molecule; 45.4 mN/m-143 Å^2/molecule) and Curosurf®:MAs (1:1 w/w):RFB2 (0.225 μM) (6.4 mN/m–804 Å^2/molecule; 24 mN/m–378 Å^2/molecule; 45 mN/m–164 Å^2/molecule).

aggregate can be observed at π≈4 mN/m. With the rise of the pressure, while the number of lipid domains increases there is a decrease in their size, emerging bright regions inside the domains. Therefore, at intermediate and higher pressures, spherical domains presenting inner small bright points that correspond to the antimycobacterial compound (RFB or RFB2) can be observed. Moreover, in the case of Curosurf® in the presence of RFB2, and especially at higher pressures, it is possible to identify domains without the antimycobacterial compound, possibly due to a "squeezing-out" of the RFB2. This is consistent with the smaller value of the A_{min} obtained for RFB2 in comparison to RFB.

The presence of the antimycobacterial compounds and higher amounts of MAs showed the occurrence of irregular and small lipid domains at intermediate and higher pressures (Fig. 4G and H). The BAM domains do not contain the characteristic bright spots of antimycobacterial compound clusters possibly due to the binding of the RFB or RFB2 to MAs when higher amounts of MAs are present at the PS monolayer. However, some filamentary structures that are possible aggregates could be observed, particularly in the presence of RFB2 (see inset of ≈24 mN/m in Fig. 4I). The appearance of these structures confirms the occurrence of immiscibility between the different components of the monolayer [14]. At lower pressures (π≈4 mN/m), and in the presence of RFB, the monolayer seems so have some condensed structures with filamentary morphology, whereas in the presence of RFB2, the monolayer is still in the LE phase. Therefore, in the presence of RFB2, the condensed domains of the monolayer occur only at intermediate and higher pressures and occupy larger areas than the obtained in the presence of RFB. However, upon compression (π≈40 mN/m), RFB seems to be present at the interface in higher proportions, as observed from the brighter domains of the monolayer (Fig. 4G).

3.3. PM-IRRAS

The PM-IRRAS of lipid/protein monolayers films, *in situ* at the air/water interface, provides unique information about the molecular structure and orientation of the film's constituents [36,58]. The results in three different regions of the isotherm (4 mN/m, 24 mN/m and 40 mN/m) are presented in Table 2.

When analyzing the PM-IRRAS band characteristic of the lipidic portion of the PS monolayer (Curosurf®), the frequency of the bands C=O and PO_2^- were, as expected, higher for π=40 mN/m than for smaller pressures (4 mN/m). Higher wavenumbers, of the carbonyl υ(C=O) stretching band (1734 cm^{-1} at π=4 mN/m and 1736 cm^{-1} at π=40 mN/m, Table 2) and the asymmetric phosphate $\upsilon_{as}(PO_2^-)$ stretching vibration (1223 cm^{-1} at π=4 mN/m and an additional band at 1249 cm^{-1} at π=40 mN/m, Table 2), correspond to the less-hydrated head groups characteristic of the LC phase that occurs at higher pressures [59]. Moreover, the dehydration of the head groups occurs not only by the compression and expulsion of water molecules at π≈40 mN/m, but also by the transition of monolayers-to-multilayers that starts roughly at this pressure, leading to the "squeezing-out" of negative lipids of the monolayer and promotion of the dehydration process. Contrastingly, at an intermediate pressure (24 mN/m), the value of $\upsilon_{as}(PO_2^-)$ stretching vibration appears to be rather low (1216 cm^{-1}) and one would expect that the compression from 4 to 24 mN/m would increase the frequency of these bands as a consequence of water molecules being expelled from the head groups upon compression. However, it has been reported that this rather unexpected low values of $\upsilon_{as}(PO_2^-)$ may occur because the phosphate moiety of the phospholipid molecules, is thought to be involved in a strong intermolecular hydrogen bonding with the glycerol hydroxyl group of neighboring molecules and these hydroxyl groups may partially mimic the solvation properties of water [59]. With the compression from π≈4 mN/m to 40 mN/m, the CH_2 asymmetrical stretching band shifts from 2926 cm^{-1} to 2915 cm^{-1} (Table 2). Hence, the decrease in the asymmetric CH_2 stretching frequency, as the monolayer is compressed, indicates the formation of *all-trans* conformation (characteristic of LC phase) and the loss of *gauche* conformers (characteristic of LE phase) [36,60,61].

The PM-IRRAS results endorse that the interaction of the MAs with the PS model is dependent of the bacterial lipid concentrations. Lower amounts of MAs do not seem to significantly interact with the head groups of the phospholipids. Independently of the amount of MAs and comparing with the PS model, the CH_2 stretching frequencies are lower at low pressures, suggesting a more ordered lipid state which might be due to the MAs residues that may be positioned within the phospholipids chains, thereby increasing the lipid packing. The CH_2 stretching is especially affected for lower concentrations of MAs, being the monolayer, in agreement to the BAM observations, condensed at all the three pressures studied. Although being more ordered at lower pressures, when the pressure increases (π≈24 and ≈40 mN/m), the monolayer of the PS model containing higher amounts of MAs is less ordered comparing to Curosurf® in the absence of MAs. Furthermore, higher frequency values obtained for the PO_2^- and C=O stretching indicate that higher amounts of MAs are responsible for the production of a less hydrated monolayer.

Both antimycobacterial compounds interact with the phospholipid head groups of the PS model, as can be confirmed by the shift induced in the PO_2^- and in the C=O bands. For RFB, at the lower surface pressures, the band contour of PO_2^- consists of at least two overlapped features, at 1211 and at 1247 cm^{-1}, probably corresponding to dihydrated and monohydrated phosphate groups, respectively. The band position

Table 2
Vibrational wavenumbers (asymmetric phosphate, carbonyl, asymmetric methylene) of the Langmuir Curosurf®, Curosurf®:MAs 9:1 w/w, Curosurf®:MAs 1:1 w/w, Curosurf®:RFB (0.118 μM), Curosurf®:RFB2 (0.225 μM), Curosurf®:MAs (1:1 w/w):RFB (0.118 μM) and Curosurf®:MAs (1:1 w/w):RFB2 (0.225 μM) monolayers on the phosphate buffer, for lower (π=4 mN/m), intermediate (π=24 mN/m) and higher pressure (π=40 mN/m).

	π=4 mN/m			π=24 mN/m			π=40 mN/m		
	$\nu(PO_2^-)$ (cm^{-1})	ν(C=O) (cm^{-1})	$\nu_{as}(CH_2)$ (cm^{-1})	$\nu(PO_2^-)$ (cm^{-1})	ν(C=O) (cm^{-1})	$\nu_{as}(CH_2)$ (cm^{-1})	$\nu(PO_2^-)$ (cm^{-1})	ν(C=O) (cm^{-1})	$\nu_{as}(CH_2)$ (cm^{-1})
Curosurf®	1223	1734	2926	1216	1730	2916	1223 1249	1736	2915
Curosurf®:MAs9:1	1220	1729	2916	1232	1728	2916	1236 1262	1731	2916
Curosurf®:MAs1:1	1259	1745	2920	1245 1263	1746	2920	1259	1744	2920
Curosurf®:RFB	1211 1247	1735	2923	1222 1250	1731	2918	1255	1741	2916
Curosurf®:RFB2	1249	1717	2921	1229	1741	2916	1253	1739	2915
Curosurf®:MAs:RFB	1213	1744	2914	1216 1242	1744	2918	1260	1744	2918
Curosurf®:MAs:RFB2	1226	1736	2919	1231	1733	2918	1237	1740	2917

at lower wavenumber suggests a high degree of hydrogen bonding between the drug and the negative lipids, containing a large number of OH groups (*e.g.* PG and possibly PI) that may mimic the solvation properties of water. The pressure increment shifts the PO_2^- band to higher wavenumbers, which is consistent with the drug being "squeezed out" from the monolayer. The interactions of the antimycobacterial compounds with the PS monolayer also occur at the fatty acid tail level, as suggested by the shift in the CH_2 wavenumbers. At lower pressures the interaction with the fatty acid tails seems to be less pronounced for RFB than for RFB2. However, both antimycobacterial compounds produce a more ordered monolayer on account of the lower wavenumbers of the CH_2 stretching obtained in the presence of the antimycobacterial compounds. The increase in the lipid order might be due to a higher packing effect by the formation of antimycobacterial compound aggregates at the interface. For intermediate and higher pressures the interactions between the antimycobacterial compounds and the PS monolayer are not so pronounced and RFB forms a less ordered monolayer than the obtained with Curosurf® alone or Curosurf® with RFB2.

Regarding the effect of RFB on PS monolayers containing MAs, it is possible to observe from PM-IRRAS data that the drug interacts with the phospholipid head groups at all the assayed pressures. At lower pressures the small frequency value of PO_2^- stretching, points to a high degree of hydrogen bonding between the drug and the negatively charged lipids, and possibly with the carboxyl and hydroxyl groups of MAs. With the pressure increase, the vibration wavenumbers of the PO_2^- are shifted to higher values. This indicates that the established hydrogen bonds are reduced, possible due to the fact of RFB being "squeezed out" from the monolayer. The resulting monolayer is condensed at all pressures but is less ordered at intermediate and higher pressures in comparison with the PS model in the absence of drug and mycolic acids. The effect of RFB2 on the PS monolayer containing high amounts of MAs is very similar to that observed for RFB. The main difference is that the frequency value of PO_2^- stretching for pressures of ≈4 mN/m is not so low, being the electrostatic interactions with the PS negatively charged lipids not so pronounced. The resultant monolayer is also condensed at the different pressures; however at smaller pressures and in the presence of higher amounts of MAs, RFB seems to form an even more ordered monolayer.

It is well known that the secondary structure of the SP-B and SP-C is related with the normal functions of these hydrophobic proteins, and changes in their structure might have a negative implication by inducing changes in the PS surface activity [62]. Accordingly, besides analyzing the lipidic portion of the PS monolayer, we have also used PM-IRRAS to study the secondary structure of the SP-B and SP-C at the dynamic inspiratory tension. In this regard we have focused on the analysis of the amide I band (1650 cm^{-1}), which is described as more sensitive to estimate the conformation and orientation of the protein compared to the amide II band (1550 cm^{-1}) [56,63]. The amide I band can therefore give information regarding the secondary structure of the proteins and according to the band position allows the identification of β-turns (1662–1682 cm^{-1}), α-helices (1645–1662 cm^{-1}), and β-sheets (1613–1637 cm^{-1}). If the band appears as two components: one at the β-sheet position and another as a shoulder at 1682–1710 cm^{-1} it is indicative of an antiparallel β-sheet. The parallel β-sheet is predicted to have higher frequency for the lower component [62,64,65]. The disorder of random coils (unstructured) occurs at the same wavenumbers of the α-helices (1637–1650 cm^{-1}), originating from the former broader and less intense bands compared to the α-helices [62,64,66]. Fig. 5 shows the effects of antimycobacterial compounds and MAs in the secondary structure of the PS proteins given by the IRRAS amide I band for π≈40 mN/m.

For the PS model, the amide I band exhibits for this pressure two overlapping bands attributed to the α-helices and β-sheet. Although the native SP-B and SP-C have α-helical segments, the secondary

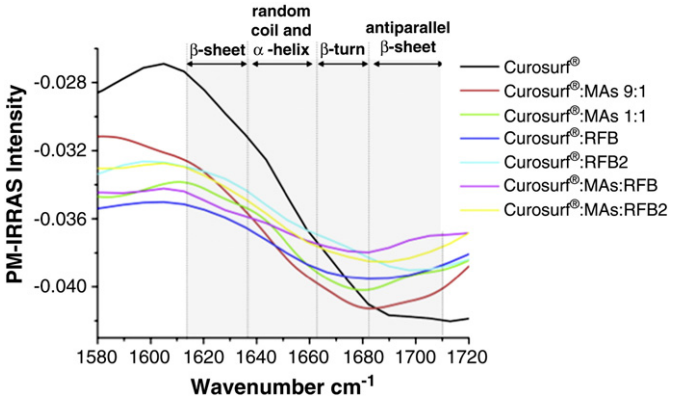

Fig. 5. PM-IRRAS spectra of Curosurf® (black line), Curosurf®:MAs 9:1 w/w (red line), Curosurf®:MAs 1:1 w/w (green line), Curosurf®:RFB (0.118 μM) (dark blue line), Curosurf®:RFB2 (0.225 μM) (light blue line), Curosurf®:MAs (1:1 w/w):RFB (0.118 μM) (purple line) and Curosurf®:MAs (1:1 w/w):RFB2 (0.225 μM) at π= 40 mN/ (yellow line).

structure is dependent of the isolation and purification procedures. Therefore, in order to conclude about the influences of other compounds in the secondary structure of the PS proteins, it is important to determine the conformation of the proteins in the conditions studied [43]. For this pressure, MAs decrease the amount of proteins at the interface, as stated by the lower intensity values of their amide I band. Higher amounts of MAs showed a more pronounced change in the secondary structure of the PS proteins. Electrostatic interactions with the proteins seem to happen, especially in the case of the presence of higher amounts of MAs as more pronounced changes are observed in the amide I stretching band. Moreover, for lower and higher amounts of MAs a decrease in absorbance centered around the α-helices region was observed. The β-turn conformation is confirmed by the presence of one peak at the 1681 cm^{-1} for lower amounts of MAs and 1678 cm^{-1} for higher amounts of MAs. Additionally, β-sheets are also formed but their amount is inferior comparing to the PS model. The interactions between RFB and the proteins of the PS model also seem to be less pronounced than the interactions between RFB2 and the proteins, probably due to the higher electrostatic repulsions verified in the former case. Although a decrease in the protein amount at the interface is confirmed in the RFB's presence, the secondary structure of the proteins does not seem to suffer a significant change as the amide I peaks assigned are similar to the ones of the Curosurf®. In the case of RFB2 interacting with the PS monolayer, the absorbance for amide I is centered around 1631, 1675 and 1700 cm^{-1} for all pressures, which is indicative of antiparallel β-sheet and β-turn conformations. When both antimycobacterial compounds and MAs are present, the PS proteins exhibit β-turns and antiparallel β-sheets. In the case of RFB, the antiparallel β-sheet has a perpendicular orientation to the air/water interface.

4. Conclusions

The PS is one of the first barriers of the lung and interacts with inhaled agents as the etiologic agent of Tb. The initial interactions of the surfactant components with the MTb may contribute to the uptake of the bacteria in alveolar epithelial cells and macrophages and subsequent initiation of adaptive immunity in the lung [43,67]. In this work, the biophysical interactions of the MTb and the antimycobacterial compounds with a PS model were evaluated, using an *in vitro* model of Langmuir monolayers. The results allowed to conclude that the amount of the MAs plays an important role in the impairment of the PS control

functions. At the dynamic inspiratory tension, with the increase of the amount of these deleterious lipids the lipid order of the PS monolayer is reduced. Since the monolayer molecular aggregation is related to the function of permeability control *via* the molecular packing [32,68], this phenomenon might be the first step in providing to the bacteria an easier access to the target, the alveolar macrophage. Hence, the lipid order decrease triggered by the high amount of MAs may contribute to the biophysical impairment of the protective PS monolayer with the consequent entrance of the bacteria into the cells due to a higher facility in reaching the alveolar macrophages. Moreover, the order decrease of the PS model is prejudicial to the lung activity, and larger quantities of MAs might largely contribute to the respiratory failure observed in chronic steps of the disease. The compounds also cause changes in the biophysical parameters of the PS, contributing RFB and RFB2 to a less compressible and more ordered monolayer. Moreover, both antimycobacterial compounds protect the PS from the lipid disordering effect caused by the higher amounts of MAs. The antimycobacterial compounds increase the order of the PS in the presence of higher amounts of MAs, and this packing increment might protect the lungs from the entry of the bacteria, being this a possible alternative explanation for the therapeutic efficiency of these antimycobacterial compounds. RFB2 also contributes to the appearance of condensed domains on the PS monolayer at very low pressures, which is indicative of an increment of the lipid order. This compound might aggregate and form monolayers, which, concerning the use of this antimycobacterial compound as a replacement therapy of atelectasis areas, could be very interesting in the future. Additionally, it is well known that a PS in normal conditions has selected properties such as high surface pressure, no hysteresis, and high compressibility of the monolayer [32,43]. The influence of the MAs and the antimycobacterial compounds in these parameters were established in order to understand the negative effects of the MAs in these parameters as well as the influence of both compounds. The MAs seem to increase the respiratory work, especially when they are present in higher quantities. The higher increment of the hysteresis associated with the lipid order decrease suggests that the bacteria could escape into the water phase, and once in the alveolar systems, be able to reach the alveolar macrophages and the bloodstream [1,53]. The secondary structure of the proteins changes upon interaction with: MAs, RFB, RFB2 and with both compounds when MAs are present. Since the antimycobacterial compounds and the MAs alter the structure of the proteins in the plateau region, the way how the material is removed from the interface also changes and this could have negative effects in the lung function and alter the normal breathing process [53,62]. Moreover, the hysteresis of the PS monolayer when both antimycobacterial compounds and MAs are present does not increase relatively to the hysteresis of the PS monolayer when MAs are present in the absence of the antimycobacterial compounds, suggesting that the RFB and its derivate might reduce the amount of bacteria that is able to reach the alveolar macrophages and the bloodstream.

Acknowledgements

Marina Pinheiro and João M. Caio thank FCT (Lisbon) for the fellowships (SFRH/BD/63318/2009 and SFRH/BD/66789/2009, respectively). Juan J. Giner-Casares acknowledges Alexander von-Humboldt foundation for a postdoctoral fellowship. Carlos Rubia-Paya is acknowledged for most valuable help during experiments. The authors thank the Spanish CICYT for financial support of this research in the framework of Projects CTQ2010-17481 and also the Junta de Andalucía (Consejería de Innovacion, Ciencia y Empresa) for special financial support (P08-FQM-4011 and P10-FQM-6703). Authors are also grateful to the FCT for financial support under projects PEst-OE/QUI/UI0612/2011 and PTDC/QUI-QUI/101022/2008 with co-participation European Community funds from the FEDER, QREN and COMPET.

References

[1] M. Pinheiro, M. Lucio, J.L. Lima, S. Reis, Liposomes as drug delivery systems for the treatment of TB, Nanomedicine (Lond) 6 (2011) 1413–1428.
[2] L.G. Dover, G.D. Coxon, Current status and research strategies in tuberculosis drug development, J. Med. Chem. 54 (2011) 6157–6165.
[3] N.R. Gandhi, P. Nunn, K. Dheda, H.S. Schaaf, M. Zignol, D. van Soolingen, P. Jensen, J. Bayona, Multidrug-resistant and extensively drug-resistant tuberculosis: a threat to global control of tuberculosis, Lancet 375 (2010) 1830–1843.
[4] A. Koul, E. Arnoult, N. Lounis, J. Guillemont, K. Andries, The challenge of new drug discovery for tuberculosis, Nature 469 (2011) 483–490.
[5] R. Figueiredo, C. Moiteiro, M.A. Medeiros, P.A. da Silva, D. Ramos, F. Spies, M.O. Ribeiro, M.C. Lourenco, I.N. Junior, M.M. Gaspar, M.E. Cruz, M.J. Curto, S.G. Franzblau, H. Orozco, D. Aguilar, R. Hernandez-Pando, M.C. Costa, Synthesis and evaluation of rifabutin analogs against Mycobacterium avium and H(37)Rv, MDR and NRP Mycobacterium tuberculosis, Bioorg. Med. Chem. 17 (2009) 503–511.
[6] Z.C. Chroneos, K. Midde, Z. Sever-Chroneos, C. Jagannath, Pulmonary surfactant and tuberculosis, Tuberculosis (Edinb) 89 (Suppl. 1) (2009) S10–S14.
[7] A.K. Agrawal, C.M. Gupta, Tuftsin-bearing liposomes in treatment of macrophage-based infections, Adv. Drug Deliv. Rev. 41 (2000) 135–146.
[8] S.M. Saad, Z. Policova, E.J. Acosta, A.W. Neumann, Effect of surfactant concentration, compression ratio and compression rate on the surface activity and dynamic properties of a lung surfactant, Biochim. Biophys. Acta 1818 (2012) 103–116.
[9] H. Zhang, Y.E. Wang, Q. Fan, Y.Y. Zuo, On the low surface tension of lung surfactant, Langmuir 27 (2011) 8351–8358.
[10] F. Bringezu, J. Ding, G. Brezesinski, A.J. Waring, J.A. Zasadzinski, Influence of pulmonary surfactant protein B on model lung surfactant monolayers, Langmuir 18 (2002) 2319–2325.
[11] U. Klenz, M. Saleem, M.C. Meyer, H.J. Galla, Influence of lipid saturation grade and headgroup charge: a refined lung surfactant adsorption model, Biophys. J. 95 (2008) 699–709.
[12] C. Alonso, T. Alig, J. Yoon, F. Bringezu, H. Warriner, J.A. Zasadzinski, More than a monolayer: relating lung surfactant structure and mechanics to composition, Biophys. J. 87 (2004) 4188–4202.
[13] G. Chimote, R. Banerjee, Effect of mycolic acid on surface activity of binary surfactant lipid monolayers, J. Colloid Interface Sci. 328 (2008) 288–298.
[14] G. Chimote, R. Banerjee, Effect of mycobacterial lipids on surface properties of Curosurf: implications for lung surfactant dysfunction in tuberculosis, Respir. Physiol. Neurobiol. 162 (2008) 73–79.
[15] Z. Wang, U. Schwab, E. Rhoades, P.R. Chess, D.G. Russell, R.H. Notter, Peripheral cell wall lipids of Mycobacterium tuberculosis are inhibitory to surfactant function, Tuberculosis (Edinb) 88 (2008) 178–186.
[16] G. Chimote, R. Banerjee, *In vitro* evaluation of inhalable isoniazid-loaded surfactant liposomes as an adjunct therapy in pulmonary tuberculosis, J. Biomed. Mater. Res. B Appl. Biomater. 94 (2010) 1–10.
[17] G. Chimote, R. Banerjee, Effect of antitubercular drugs on dipalmitoylphosphatidylcholine monolayers: implications for drug loaded surfactants, Respir. Physiol. Neurobiol. 145 (2005) 65–77.
[18] A. Kurashima, T. Mori, Y. Tomono, S. Abe, M. Nagaoka, M. Abe, A new anti-mycobacterial agent, rifabutin, Kekkaku 85 (2010) 743–756.
[19] P.A. Aristoff, G.A. Garcia, P.D. Kirchhoff, H.D. Hollis Showalter, Rifamycins — obstacles and opportunities, Tuberculosis (Edinb) 90 (2010) 94–118.
[20] Z. Zhang, Y. Pen, R.G. Edyvean, S.A. Banwart, R.M. Dalgliesh, M. Geoghegan, Adhesive and conformational behaviour of mycolic acid monolayers, Biochim. Biophys. Acta 1798 (2010) 1829–1839.
[21] P. Draper, The outer parts of the mycobacterial envelope as permeability barriers, Front. Biosci. 3 (1998) D1253–D1261.
[22] M. Villeneuve, M. Kawai, M. Watanabe, Y. Aoyagi, Y. Hitotsuyanagi, K. Takeya, H. Gouda, S. Hirono, D.E. Minnikin, H. Nakahara, Differential conformational behaviors of alpha-mycolic acids in Langmuir monolayers and computer simulations, Chem. Phys. Lipids 163 (2010) 569–579.
[23] M. Villeneuve, M. Kawai, M. Watanabe, Y. Aoyagi, Y. Hitotsuyanagi, K. Takeya, H. Gouda, S. Hirono, D.E. Minnikin, H. Nakahara, Conformational behavior of oxygenated mycobacterial mycolic acids from Mycobacterium bovis BCG, Biochim. Biophys. Acta 1768 (2007) 1717–1726.
[24] K. Takayama, C. Wang, G.S. Besra, Pathway to synthesis and processing of mycolic acids in Mycobacterium tuberculosis, Clin. Microbiol. Rev. 18 (2005) 81–101.
[25] Y.Y. Zuo, R.A. Veldhuizen, A.W. Neumann, N.O. Petersen, F. Possmayer, Current perspectives in pulmonary surfactant — inhibition, enhancement and evaluation, Biochim. Biophys. Acta 1778 (2008) 1947–1977.
[26] P. Ludwiczak, M. Gilleron, Y. Bordat, C. Martin, B. Gicquel, G. Puzo, Mycobacterium tuberculosis phoP mutant: lipoarabinomannan molecular structure, Microbiology 148 (2002) 3029–3037.
[27] Y. Benadie, M. Deysel, D.G. Siko, V.V. Roberts, S. Van Wyngaardt, S.T. Thanyani, G. Sekanka, A.M. Ten Bokum, L.A. Collett, J. Grooten, M.S. Baird, J.A. Verschoor, Cholesteroid nature of free mycolic acids from M. tuberculosis, Chem. Phys. Lipids 152 (2008) 95–103.
[28] Y.Y. Zuo, M. Ding, D. Li, A.W. Neumann, Further development of Axisymmetric Drop Shape Analysis-captive bubble for pulmonary surfactant related studies, Biochim. Biophys. Acta 1675 (2004) 12–20.
[29] H. Zhang, Q. Fan, Y.E. Wang, C.R. Neal, Y.Y. Zuo, Comparative study of clinical pulmonary surfactants using atomic force microscopy, Biochim. Biophys. Acta 1808 (2011) 1832–1842.
[30] X. Chen, Z. Huang, W. Hua, H. Castada, H.C. Allen, Reorganization and caging of DPPC, DPPE, DPPG, and DPPS monolayers caused by dimethylsulfoxide observed using Brewster angle microscopy, Langmuir 26 (2010) 18902–18908.

[31] L.A. Creuwels, E.H. Boer, R.A. Demel, L.M. van Golde, H.P. Haagsman, Neutralization of the positive charges of surfactant protein C. Effects on structure and function, J. Biol. Chem. 270 (1995) 16225–16229.
[32] N. Aydogan, B. Uslu, H. Tanaci, Biophysical investigation of the interfacial properties of cationic fluorocarbon/hydrocarbon hybrid surfactant: mimicking the lung surfactant protein C, J. Colloid Interface Sci. 360 (2011) 163–174.
[33] M. Ross, S. Krol, A. Janshoff, H.J. Galla, Kinetics of phospholipid insertion into monolayers containing the lung surfactant proteins SP-B or SP-C, Eur. Biophys. J. 31 (2002) 52–61.
[34] S.G. Taneva, K.M. Keough, Calcium ions and interactions of pulmonary surfactant proteins SP-B and SP-C with phospholipids in spread monolayers at the air/water interface, Biochim. Biophys. Acta 1236 (1995) 185–195.
[35] J. Perez-Gil, C. Casals, D. Marsh, Interactions of hydrophobic lung surfactant proteins SP-B and SP-C with dipalmitoylphosphatidylcholine and dipalmitoylphosphatidylglycerol bilayers studied by electron spin resonance spectroscopy, Biochemistry 34 (1995) 3964–3971.
[36] R. Mendelsohn, G. Mao, C.R. Flach, Infrared reflection-absorption spectroscopy: principles and applications to lipid–protein interaction in Langmuir films, Biochim. Biophys. Acta 1798 (2010) 788–800.
[37] R.M. de Oliveira, J. Ferreira, M.J. Santos, R.M. Faria, O.N. Oliveira Jr., Probing the functionalization of gold surfaces and protein adsorption by PM-IRRAS, Chemphyschem 12 (2011) 1736–1740.
[38] S. Schurch, H. Bachofen, F. Possmayer, Surface activity *in situ*, *in vivo*, and in the captive bubble surfactometer, Comp. Biochem. Physiol. A Mol. Integr. Physiol. 129 (2001) 195–207.
[39] S.M. Saad, Z. Policova, E.J. Acosta, M.L. Hair, A.W. Neumann, Mixed DPPC/DPPG monolayers at very high film compression, Langmuir 25 (2009) 10907–10912.
[40] K.Y. Lee, Collapse mechanisms of Langmuir monolayers, Annu. Rev. Phys. Chem. 59 (2008) 771–791.
[41] S. Schurch, H. Bachofen, J. Goerke, F. Possmayer, A captive bubble method reproduces the *in situ* behavior of lung surfactant monolayers, J. Appl. Physiol. 67 (1989) 2389–2396.
[42] H. Bachofen, S. Schurch, Alveolar surface forces and lung architecture, Comp. Biochem. Physiol. A Mol. Integr. Physiol. 129 (2001) 183–193.
[43] R. Wustneck, J. Perez-Gil, N. Wustneck, A. Cruz, V.B. Fainerman, U. Pison, Interfacial properties of pulmonary surfactant layers, Adv. Colloid Interface Sci. 117 (2005) 33–58.
[44] C. Nunes, G. Brezesinski, C. Pereira-Leite, J.L. Lima, S. Reis, M. Lucio, NSAIDs interactions with membranes: a biophysical approach, Langmuir 27 (2011) 10847–10858.
[45] Z. Wang, S. Yang, Effects of fullerenes on phospholipid membranes: a Langmuir monolayer study, Chemphyschem 10 (2009) 2284–2289.
[46] J. Perez-Gil, T.E. Weaver, Pulmonary surfactant pathophysiology: current models and open questions, Physiology (Bethesda) 25 (2010) 132–141.
[47] T. Ivanova, I. Minkov, I. Panaiotov, P. Saulnier, J.E. Proust, Dilatational properties and morphology of surface films spread from clinically used lung surfactants, Colloid Polym. Sci. 282 (2004) 1258–1267.
[48] T. Gross, E. Zmora, Y. Levi-Kalisman, O. Regev, A. Berman, Lung-surfactant–meconium interaction: *in vitro* study in bulk and at the air-solution interface, Langmuir 22 (2006) 3243–3250.
[49] H. Zhang, Y.E. Wang, C.R. Neal, Y.Y. Zuo, Differential effects of cholesterol and budesonide on biophysical properties of clinical surfactant, Pediatr. Res. 71 (2012) 316–323.
[50] C. Alonso, A. Waring, J.A. Zasadzinski, Keeping lung surfactant where it belongs: protein regulation of two-dimensional viscosity, Biophys. J. 89 (2005) 266–273.
[51] G. Chimote, R. Banerjee, Lung surfactant dysfunction in tuberculosis: effect of mycobacterial tubercular lipids on dipalmitoylphosphatidylcholine surface activity, Colloids Surf. B Biointerfaces 45 (2005) 215–223.
[52] R. Almog, C.A. Mannella, Molecular packing of cord factor and its interaction with phosphatidylinositol in mixed monolayers, Biophys. J. 71 (1996) 3311–3319.
[53] R.K. Harishchandra, M. Saleem, H.J. Galla, Nanoparticle interaction with model lung surfactant monolayers, J. R. Soc. Interface 7 (Suppl. 1) (2010) S15–S26.
[54] V.V. Vostrikov, A.A. Selishcheva, G.M. Sorokoumova, Y.N. Shakina, V.I. Shvets, O.Y. Savel'ev, V.I. Polshakov, Distribution coefficient of rifabutin in liposome/water system as measured by different methods, Eur. J. Pharm. Biopharm. 68 (2008) 400–405.
[55] T. Schmidt, L. Caseli, T. Nobre, M. Zaniquelli, O. Oliveira Jr., Interaction of horseradish peroxidase with Langmuir monolayers of phospholipids, Colloids Surf. A Physicochem. Eng. Asp. 321 (2008) 206–210.
[56] M. Allouche, S. Castano, D. Colin, B. Desbat, B. Kerfelec, Structure and orientation of pancreatic colipase in a lipid environment: PM-IRRAS and Brewster angle microscopy studies, Biochemistry 46 (2007) 15188–15197.
[57] A.M. Goncalves da Silva, R.I. Romao, Mixed monolayers involving DPPC, DODAB and oleic acid and their interaction with nicotinic acid at the air–water interface, Chem. Phys. Lipids 137 (2005) 62–76.
[58] C.R. Flach, A. Gericke, R. Mendelsohn, Quantitative determination of molecular chain tilt angles in monolayer films at the air/water interface: infrared reflection/absorption spectroscopy of behenic acid methyl ester, J. Phys. Chem. B 101 (1997) 58–65.
[59] A. Dicko, H. Bourque, M. Pézolet, Study by infrared spectroscopy of the conformation of dipalmitoylphosphatidylglycerol monolayers at the air–water interface and transferred on solid substrates, Chem. Phys. Lipids 96 (1998) 125–139.
[60] K. Czapla, B. Korchowiec, E. Rogalska, Differentiating oxicam nonsteroidal anti-inflammatory drugs in phosphoglyceride monolayers, Langmuir 26 (2010) 3485–3492.
[61] D.G. Cameron, E.F. Gudgin, H.H. Mantsch, Dependence of acyl chain packing of phospholipids on the head group and acyl chain length, Biochemistry 20 (1981) 4496–4500.
[62] P.C. Stenger, C. Alonso, J.A. Zasadzinski, A.J. Waring, C.L. Jung, K.E. Pinkerton, Environmental tobacco smoke effects on lung surfactant film organization, Biochim. Biophys. Acta 1788 (2009) 358–370.
[63] O.G. Travkova, J. Andra, H. Mohwald, G. Brezesinski, Conformational properties of arenicins: from the bulk to the air–water interface, Chemphyschem 11 (2010) 3262–3268.
[64] A. Banc, B. Desbat, D. Renard, Y. Popineau, C. Mangavel, L. Navailles, Structure and orientation changes of omega- and gamma-gliadins at the air-water interface: a PM-IRRAS spectroscopy and Brewster angle microscopy study, Langmuir 23 (2007) 13066–13075.
[65] J. Kubelka, T.A. Keiderling, Differentiation of beta-sheet-forming structures: *ab initio*-based simulations of IR absorption and vibrational CD for model peptide and protein beta-sheets, J. Am. Chem. Soc. 123 (2001) 12048–12058.
[66] S. Venyaminov, N.N. Kalnin, Quantitative IR spectrophotometry of peptide compounds in water (H2O) solutions. I. Spectral parameters of amino acid residue absorption bands, Biopolymers 30 (1990) 1243–1257.
[67] Z.C. Chroneos, K. Midde, Z. Sever-Chroneos, C. Jagannath, Pulmonary surfactant and tuberculosis, Tuberculosis (Edinb) 89 (2009) 10–14.
[68] T. Hasegawa, R.M. Leblanc, Aggregation properties of mycolic acid molecules in monolayer films: a comparative study of compounds from various acid-fast bacterial species, Biochim. Biophys. Acta 1617 (2003) 89–95.